

# Design of a Highly Stable and Uniform Thermal Test Facility for MGRS Development

**Sei Higuchi, Ke-Xun Sun, Daniel B. DeBra, Saps Buchman, Robert L. Byer**

Hansen Experimental Physics Laboratory, Stanford University, 452 Lomita Mall, Stanford, CA 94305, USA

E-mail: [seihiguchi@stanford.edu](mailto:seihiguchi@stanford.edu)

**Abstract.** We have designed combined passive and active thermal control system to achieve sub microkelvin temperature stability and uniformity over an optics bench size enclosure, which has an analogous structure to the LISA spacecraft. For the passive control, we have constructed a new thermal enclosure that has a multilayer structure with alternative conducting and insulating layers, which enables the temperature uniformity and ease the burden of the active control. The thermal enclosure becomes an important test facility for Modular Gravitational Reference Sensor (MGRS) development. For the active control, we have developed a model predictive control (MPC) algorithm, which will regulate temperature variations of the proof-mass (PM) down to sub-microkelvin over the LISA science band. The LISA mission requires extremely tight temperature control, which is as low as  $30 \mu K/\sqrt{Hz}$  over  $0.1 mHz$  to  $1 Hz$ . Both temporal stability and spatial uniformity in temperature must be achieved. Optical path length variations on optical bench must be kept below  $40 pm/\sqrt{Hz}$  over  $0.1 mHz$  to  $1 Hz$ . Temperature gradient across the proof mass housing also must be controlled to reduce differential thermal pressure. Thermal disturbances due to, for example, solar radiation and heat generation from electronics, are expected to be significant disturbance source to the LISA sensitivity requirements. The MGRS will alleviate the thermal requirement due to its wider gap between the proof-mass and the housing wall. However, a thermally stable and uniform environment is highly desirable to achieve more precise science measurement for future space science missions.

## 1. Introduction

This research focuses on developing a thermal test facility for modular gravitational reference sensor (MGRS) ground verification testing. It aims to provide thermal stability better than  $30 \mu K/\sqrt{Hz}$  over  $0.1 mHz$  to  $1 Hz$  by taking advantage of active control. Its extension is suitable for in-flight thermal control for the LISA spacecraft to compensate solar radiation. Limited thermal mass of the LISA spacecraft and relatively low frequency range in which LISA is interested, the spacecraft calls for active compensation mechanism to satisfy the thermal requirements. In addition to stability, thermal gradient across the proof mass housing needs to be minimized to avoid differential radiation pressure. Thus, spatial uniformity is also important to fully ensure LISA's strain sensitivity. The graphical interpretation of the thermal stability goal is shown in Figure 1. Spectral temperature variations is drawn in the figure. The primarily goal of control system is to push down the curve below the LISA thermal requirement region by both passive insulation and active control.

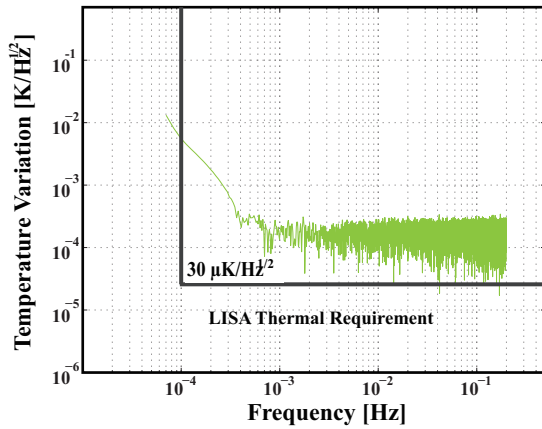


**Figure 1.** Graphical interpretation of thermal requirement. We aim to push the spectral curve below the thermal requirement by passive insulation and active control.

Thermal disturbances including solar radiation, and temperature gradients across the proof mass housing is expected to be significant disturbance source to the LISA sensitivity requirements. Even a small temperature gradient can produce distortions in the housing structure, which results in a change in the mass attraction force [7]. Temperature fluctuations also cause radiometer effects with residual gas pressure. Lastly, the fluctuations in the temperature gradient across the proof-mass housing will cause the differential thermal radiation pressure that adds extra acceleration to proof mass. P. L. Bender[1] claims that the passive thermal isolation clearly will become worse at frequencies substantially below 0.1  $mHz$  and suggests the need of active temperature control system as well as larger gaps around the proof-mass. the current nominal gap size is 2  $mm$ [8] while the MGRS gap size is an order of a few cm [4, 5, 6].

The LISA spacecraft must reject non-gravitational-wave forces, since the gravitational waves reaching to the vicinity of the Earth have a very small amplitude. Minimizing the non-gravitational-wave accelerations, which come from both the environment and the spacecraft themselves, is the task of MGRS for drag-free control. The main environmental disturbances to LISA are the forces from the Sun: fluctuations in solar radiation pressure and pressure from the solar wind. The job of the spacecraft is to shield an internal proof mass that floats freely, not attached to the spacecraft, from external disturbances.

## 2. Design of highly stable and uniform thermal chamber

Figure 2 shows the overview of the experimental system. We have a thermal enclosure specially designed for ground testing, which simulates the LISA spacecraft flying in the deep space. Heating pads and temperature sensors are attached around the enclosure. They are connected to a computer through GPIB interface. Python-based software controls experiment and also logs data.

The left of Figure 3 demonstrates a schematic of the thermal chamber. The top part corresponds to the spacecraft's solar panel module that are made of aluminum honeycomb, polyimide and carbon fiber reinforce plastic (CFRP). However, both polyimide and CFRP are not available at reasonable prices, they are replaced by polystyrene form and acrylic sheets. They have similar thermal properties. On the very top of the solar module part, six heating pads are mounted over a 2-mm-thick copper sheet so that we can simulate solar radiation heat

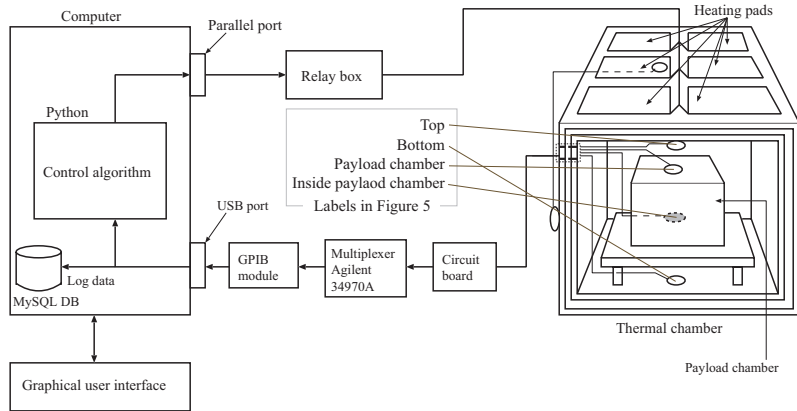


**Figure 2.** Overview of the thermal experimental system

input to spacecraft. The heating pads are covered with air bubble sheet to reduce wasted heat dissipation to air. These heating pads are powerful enough to simulate the solar constant,  $1350 \text{ W/m}^2$ . All heating pads are connected to an external mechanical relay box and controlled via the computer. The top view of the thermal chamber and a door are shown on the right.

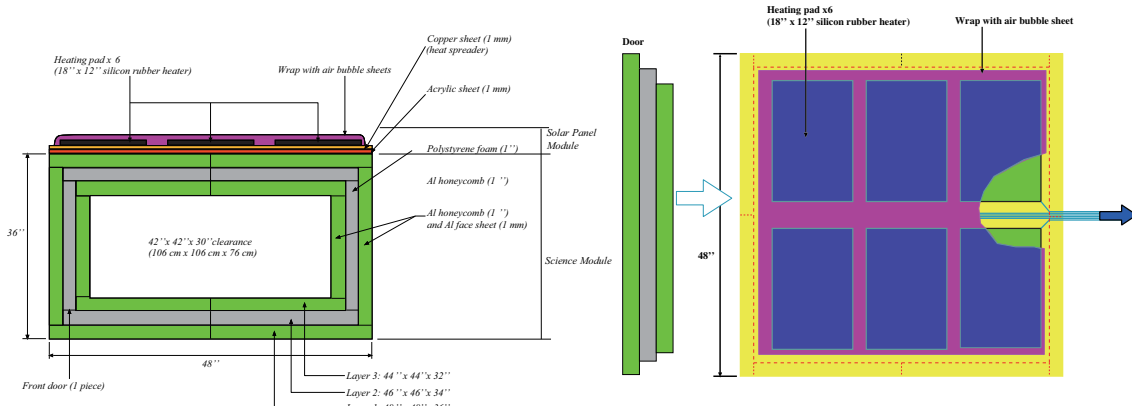


**Figure 3.** Schematic of the new thermal chamber: side view (left) and top view (right).

The bottom part is associated with the science module of the LISA spacecraft, which we plant to place optics system, MGRS test-object, and also conduct active control. In the space environment, because there is not convective heat transfer, thermal coupling will be weaker than the lab environment. However, we anticipate the metal structure won't have enough temperature attenuation capability particularly at the lower frequency range. Therefore, we decided to design a multi-layer structure blended with aluminum honeycomb and polystyrene form. The very outer layer, which is made of 1-inch thick aluminum honeycomb and 2-mm thick aluminum face sheets, provides first order temperature uniformity particularly along the face sheets. Honeycomb structure makes the whole system significantly lighter and also works as a thermal insulation. Then the polystyrene-form layer attenuates temperature fluctuations. The third layer completes a sealed control volume as a heat spreader that equalize temperature profile around the inner space of the chamber. The whole chamber is placed on a 8-feet by 4-feet optics table that simulates the cold plate of the spacecraft. Finally, the entire experimental system is

placed within a clear plastic thermal tent, primarily to cut down on air drafts. A small chamber is placed inside the new chamber that simulates the Y-tube telescope of the LISA spacecraft. It is referred as a payload chamber. The completed chamber appears in Figure 4.



**Figure 4.** New thermal chamber constructed at Stanford University

### 3. Dynamic characteristics against disturbance temperature input

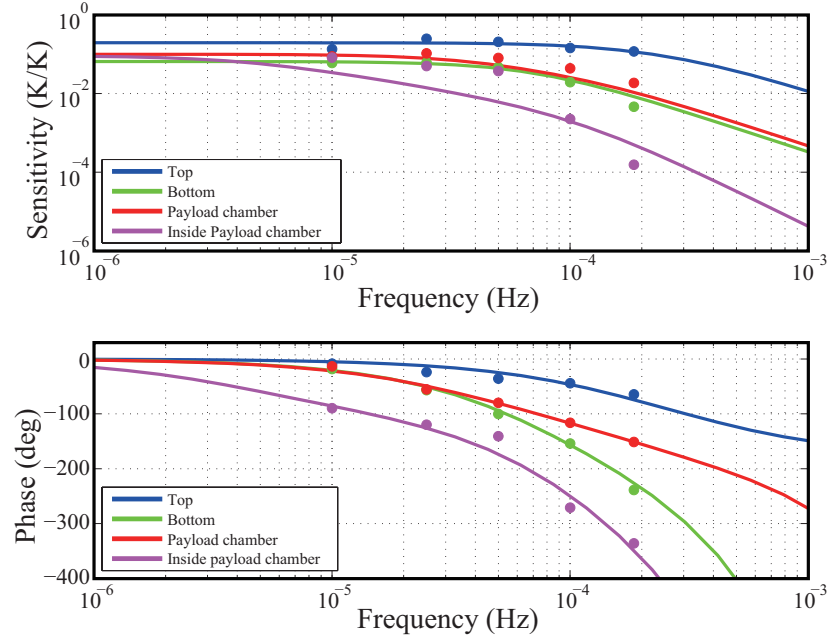
The Figure 5 demonstrates the dynamic characteristics of the new thermal chamber against the disturbance input. The disturbance sinusoidal input is applied by the heating pads at various frequencies. Output temperature is measured at four locations indicated in Figure 2. The experimental data is fitted as a second or third-order LTI model with a time-delay element. The sensitivity inside the payload chamber is  $2.2 \times 10^{-3}$  at  $0.1 \text{ mHz}$ . Table 1 shows the zero-frequency gain, time-delays and time constants (T.C.). New multi-layer structure chamber enables to achieve lower sensitivity to disturbance input at the frequency range of LISA's interest.

**Table 1.** Key parameters of the dynamic characteristics

Parts	Zero frequency gain (K/K)	Time-delay (sec)	T.C. 1 (sec)	T.C. 2 (sec)	T.C. 3 (sec)
Top	$1.9585 \times 10^{-1}$	$7.6422 \times 10^{-5}$	$2.5047 \times 10^3$	$6.2663 \times 10^3$	none
Bottom	$6.5523 \times 10^{-2}$	$8.2531 \times 10^3$	$1.4059 \times 10^4$	$1.4096 \times 10^4$	none
Cu chamber	$9.9816 \times 10^{-2}$	$1.7701 \times 10^3$	$7.0631 \times 10^3$	$2.9948 \times 10^4$	none
Inside	$9.0222 \times 10^{-2}$	$1.3148 \times 10^4$	$8.4859 \times 10^3$	$1.3148 \times 10^4$	$2.4117 \times 10^5$

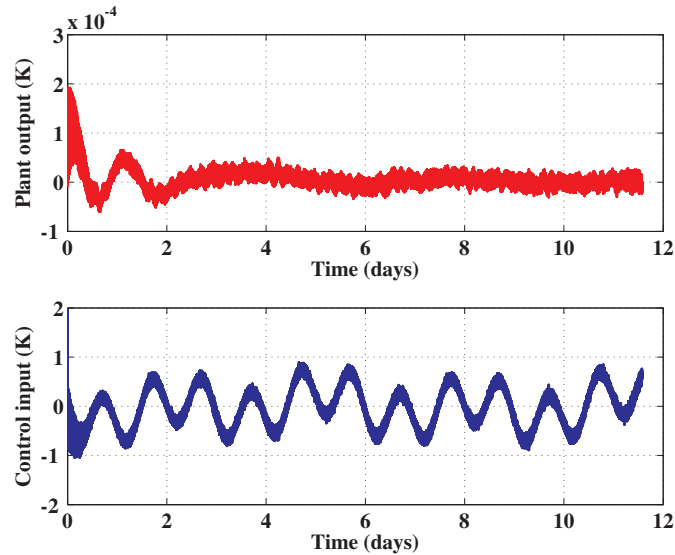
### 4. Results: active control simulation and experimental spectral stability performance of the new chamber

Figure 6 demonstrates a 12-day simulation of the proof-mass temperature being controlled with the MPC algorithm applied the LTI model obtained previously. The control input is also shown. The simulation accounts for  $50 \mu\text{K}/\sqrt{\text{Hz}}$  of sensor noise added at the plant output. The temperature is maintained approximately  $\pm 20 \mu\text{K}$  at steady-state. During the simulation, the disturbance temperature was modeled as a combination of sinusoidal functions,



**Figure 5.** Bode plot: solid line fitted LTI model. Dots represent experimental data points.

$d(t) = \sum_{i=1}^3 A_i \sin(\omega_i t + \phi_i)$  and Gaussian random noise. The controller did not have any information of the disturbance's parameters (frequency, phase, and amplitude) at  $t = 0$ . The controller adaptively estimates the unknown parameters of disturbance.



**Figure 6.** Simulation results of active control

Figure 7 compares the root mean squared spectral density (amplitude spectral density, ASD) of temperature variations of the proof-mass, the new thermal chamber, and the old thermal chamber. The proof-mass data is simulation shown in Figure 6 while thermal chamber data is

obtained through experiment. The spectral stability of the new chamber has been improved nearly by an order of magnitude at 1 mHz over the old chamber. Finally, the expected thermal stability will be below  $30 \mu K/\sqrt{Hz}$  above 0.1 mHz with the aid of active control.

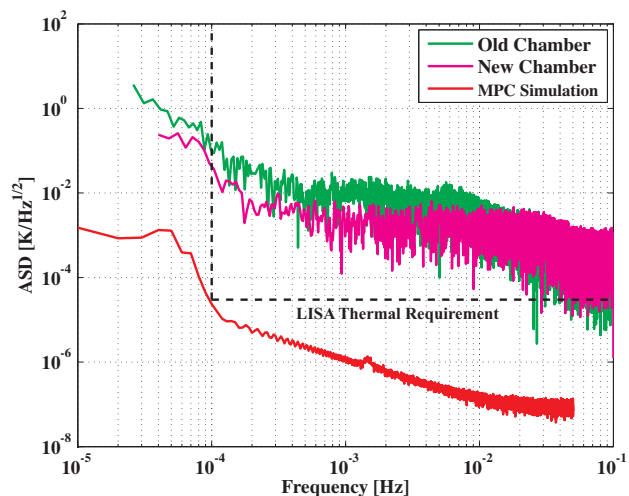


**Figure 7.** Spectral thermal stability of the new and old thermal chamber (experiment) and active control result (simulation). The below of dashed lines indicates the LISA thermal requirement:  $30 \mu K/Hz^{1/2}$ .

## 5. Conclusion

The experimental performance of the new multi-layer thermal chamber and the active control simulation results have demonstrated the potential of satisfying the LISA thermal stability requirement. Continuing development will achieve more precision.

## 6. Acknowledgments

This research was supported by NASA, NNX07AK65G, Modular Gravitational Reference Sensor for Space Gravitational Wave Detection, and Department of Aeronautics & Astronautics, Stanford University. Authors also would like to acknowledge Mark McKelvey, Fred Witteborn at NASA Ames Research Center, and Hansen Experimental Physics Laboratory at Stanford University.

## References

- [1] Bender P 2003 *Class. Quantum Grav.* **20** S301
- [2] Buckman S et al 2004 *5th International LISA Symposium, ESTEC*
- [3] Sun K, Allen G, Buchman S, DeBra D and Byer R 2005 *Class. Quantum Grav.* **22** 10 S287
- [4] Sun K, Allen G, Williams S, Buchman S, DeBra D, Byer R 2006 *Journal of Physics CS* **32** 137
- [5] Sun K et al 2006 *AIP Conference Proceedings* **873** 515
- [6] Sun K, Johann U, DeBra D, Buchman S, Byer R 2007 *Journal of Physics: Conference Series* **60** 272
- [7] Swank A 2006 *Class. Quantum Grav.* **23** 3437
- [8] Astrium 2006 *LISA Final Technical Report* **LI-RP-DS-009**